Coupling Local and Global Shape Optimization in Aerodynamic Design

Régis Duvigneau

INSTITUT NATIONAL DE RECHERCHE EN INFORMATIQUE ET EN AUTOMATIQUE

Coupling Local and Global Shape Optimization in Aerodynamic Design

R. Duvigneau

N° 7684

July 2011

Domaine 1

ISSN 0249-6399 ISRN INRIA/RR--7684--FR+ENG

INSTITUT NATIONAL
DE RECHERCHE
EN INFORMATIQUE
ET EN AUTOMATIQUE

INRIA

centre de recherche
SOPHIA ANTIPOLIS - MÉDITERRANÉE

Coupling Local and Global Shape Optimization in Aerodynamic Design

R. Duvigneau *

Domaine : Mathématiques appliquées, calcul et simulation
Équipes-Projets Opale

Rapport de recherche n° 7684 — July 2011 — 23 pages

Abstract: Wing design in aerodynamics requires the definition of global geometrical characteristics, such as span, root/tip length ratio, angle of attack, twist angle, sweep angle, etc, as well as local geometrical features that determine the wing section. The objective of this study is to propose an efficient algorithm to achieve the optimization of both global and local shape parameters. We consider as testcase the drag minimization, under lift constraint, of the wing shape of a business aircraft in transonic regime, the flow being modeled by the compressible Euler equations.
We show that a straightforward optimization of all parameters fails, due to multimodality of the optimization problem. Then, some alternative strategies are proposed. Among them, the use of virtual Nash games yields the best results, in terms of cost function value obtained as well as computational efficiency.

Key-words: Aerodynamics, design, optimization, Nash games

* INRIA Opale Project-Team

Centre de recherche INRIA Sophia Antipolis – Méditerranée
2004, route des Lucioles, BP 93, 06902 Sophia Antipolis Cedex
Téléphone : +33 4 92 38 77 77 — Télécopie : +33 4 92 38 77 65

Couplage d'optimisation de forme locale et globale en conception aérodynamique

Résumé : La conception de voilure en aérodynamique nécessite la définition de caractéristiques géométriques globales, telles l'envergure, le rapport des longueurs à l'emplanture et saumon, les angles d'attaque, de torsion, de flèche, etc, ainsi que des caractéristiques géométriques locales qui déterminent une section de l'aile. L'objectif de cette étude est de proposer un algorithme efficace pour réaliser l'optimisation des paramètres de forme globaux et locaux. On considère comme cas-test la minimisation de traînée, sous contrainte de portance, de la forme de l'aile d'un jet d'affaires en régime transsonique, l'écoulement étant modélisé par les équations d'Euler compressible.
On montre qu'une optimisation directe de tous les paramètres échoue, à cause de la multimodalité du problème. Par suite, on propose plusieurs stratégies alternatives. Parmi celles-ci, l'utilisation de jeux de Nash virtuels aboutit au meilleur résultat, en termes de valeur obtenue pour la fonction coût et d'efficacité de calcul.

Mots-clés : Aérodynamique, conception, optimisation, Jeu de Nash

1 Introduction

Wing design in aerodynamics requires the definition of global geometrical characteristics, such as span, root/tip length ratio, angle of attack, twist angle, sweep angle, etc, as well as local geometrical features that determine the wing section. Numerical optimization based on flow simulations plays now a significant role in the design procedure. Then, optimization algorithms are used to determine these global and local shape parameters. However, these tasks are commonly carried out in an independent way, possibly using different flow models. Thus, studies related to the simultaneous optimization of global and local shape parameters are not easily found in the literature.

Therefore, the objective of this work is to study how to achieve the optimization of a wing shape including both global and local parameters and propose some efficient algorithms. The testcase considered for this study is the drag minimization, under lift constraint, of the wing shape of a business aircraft in transonic regime. The flow is modeled by the three-dimensional compressible Euler equations.

In first sections, we briefly present the simulation methods employed to simulate the flow and the geometrical model used for the wing shape, including both global and local parameters. Then, a straightforward optimization of all parameters is carried out. Poor results are obtained and alternative strategies are proposed, namely *nested optimizations*, *successive optimizations* and *virtual Nash game*. Results obtained are analyzed, in terms of cost function value, computational efficiency, wing shape and flow fields.

2 Aerodynamic analysis

2.1 Modeling

This study is restricted to three-dimensional inviscid compressible flows governed by the Euler equations. Then, the state equations can be written in the conservative form :

$$\frac{\partial W}{\partial t} + \frac{\partial F_1(W)}{\partial x} + \frac{\partial F_2(W)}{\partial y} + \frac{\partial F_3(W)}{\partial z} = 0, \tag{1}$$

where $W = (\rho, \rho u, \rho v, \rho w, E)$ are the conservative flow variables, with ρ the density, $\overrightarrow{U} = (u, v, w)$ the velocity vector and E the total energy per unit of volume, and $\overrightarrow{F} = (F_1(W), F_2(W), F_3(W))$ is the vector of the convective fluxes. The pressure p is obtained from the perfect gas state equation $p = (\gamma - 1)(E - \frac{1}{2}\rho \| \overrightarrow{U} \|^2)$, where $\gamma = 1.4$ is the ratio of the specific heat coefficients.

2.2 Spatial discretization

Provided that the flow domain Ω is discretized by a tetrahedrization $\mathcal{T}_h$, a discretization of equation (1) at the mesh node s_i is obtained by integrating (1) over the volume C_i, that is built around the node s_i by joining barycenters of the tetrahedra and triangles containing s_i and midpoints of the edges adjacent to s_i :

$$Vol_i \frac{\partial W_i}{\partial t} + \sum_{j \in N(i)} \Phi(W_i, W_j, \overrightarrow{\eta}_{ij}) = 0, \tag{2}$$

where W_i represents the cell averaged state and Vol_i the volume of the cell C_i. $N(i)$ is the set of the neighboring nodes. $\Phi(W_i, W_j, \overrightarrow{\eta}_{ij})$ is an approximation of the integral of the fluxes $\overrightarrow{F}$ over the boundary ∂C_{ij} between C_i and C_j, which depends on W_i, W_j and $\overrightarrow{\eta}_{ij}$ the integral of a unit normal vector over ∂C_{ij}. These numerical fluxes are evaluated using upwinding, according to the approximate Riemann solver HLLC [3].

A high order scheme is obtained by interpolating linearly the physical variables from s_i to the midpoint of $[s_i s_j]$, before equation (2) is employed to evaluate the fluxes. Nodal gradients are obtained from a weighting average of the P1 Galerkin gradients computed on each tetrahedron containing s_i. In order to avoid spurious oscillations of the solution in the vicinity of the shock, a slope limitation procedure using the Barth-Jespersen limiter [2] is introduced. The resulting discretization scheme exhibits a high-order accuracy in the regions where the solution is regular.

2.3 Time integration

A first order implicit backward scheme is employed for the time integration of (2), which yields :

$$\frac{Vol_i}{\Delta t} \delta W_i + \sum_{j \in N(i)} \Phi(W_i^{n+1}, W_j^{n+1}, \overrightarrow{\eta}_{ij}) = 0, \tag{3}$$

with $\delta W_i = W_i^{n+1} - W_i^n$. Then, the linearization of the numerical fluxes provides the following integration scheme :

$$\left(\frac{Vol_i}{\Delta t} + J_i^n\right) \delta W_i = - \sum_{j \in N(i)} \Phi(W_i^n, W_j^n, \overrightarrow{\eta}_{ij}). \tag{4}$$

Here, J_i^n is the jacobian matrix of the first-order numerical flux of Lax-Friedrichs [7], whereas the right hand side of (4) is evaluated using high-order approximations. The resulting integration scheme provides a high-order solution of the steady-state problem.

3 Aerodynamic design optimization

A simulation-based shape optimization problem consists of minimizing a cost function $\mathcal{J}$, which depends on a shape Γ and state variables W. In parametric approaches, the shape Γ is defined by a small number of design variables $\mathbf{x} = (x_i)_{i=1,\dots,n}$, which are considered as optimization variables. The use of such a parametric approach allows to replace the initial shape optimization problem of infinite dimension by a problem with a finite number n of unknowns. State variables W (i.e. physical flow fields) depend implicitly on the design variables through the state equations $\mathcal{E}(\mathbf{x}, W(\mathbf{x})) = 0$. Finally, a general parametric shape optimization problem can be expressed as :

$$\begin{aligned} &\text{Minimize } \mathcal{J}(\mathbf{x}, W(\mathbf{x})) \quad \mathbf{x} \in \Re^n, \\ &\text{Subject to } \mathcal{C}(\mathbf{x}, W(\mathbf{x})) \leq 0, \end{aligned} \tag{5}$$

where $\mathcal{C}$ represents additional (physical or geometrical) constraints.

Several optimization strategies and numerical methods can be carried out to solve such a problem. Nevertheless, a typical algorithm can be described as follows:

1. choose initial design variables $\mathbf{x}^{(0)}$;
   $k \leftarrow 0$;
2. begin iteration k of the optimization loop ;
3. solve the state equations $\mathcal{E}(\mathbf{x}^{(k)}, W(\mathbf{x}^{(k)})) = 0$ yielding the state variables $W(\mathbf{x}^{(k)})$;
4. estimate the cost function $\mathcal{J}(\mathbf{x}^{(k)}, W(\mathbf{x}^{(k)}))$;
5. update the design variables to $\mathbf{x}^{(k+1)}$ according to the optimization algorithm ;
6. finish iteration k of the optimization loop ;
   if a stopping criterion is reached then STOP ;
   else $k \leftarrow k + 1$ GOTO step (2).

In this study, we consider a typical problem of wing shape design, which consists of minimizing the drag coefficient C_D of a wing, while maintaining a constant lift coefficient C_L. If one considers the lift constraint within a penalty method, the following cost function is finally used :

$$\mathcal{J}(\mathbf{x}) = C_D + \rho \max(0\,; C_L^{ref} - C_L), \tag{6}$$

where ρ is a penalty parameter to be calibrated and C_L^{ref} the reference lift coefficient. For this study, we choose $\rho = 10^4$.

The design optimization algorithm presented above is carried out on the basis of the CMA-ES (Covariance Matrix Adaption Evolution Strategy) optimizer [5], which is known for its robustness and efficiency for multimodal problems.

4 Global / local wing shape parameterization

The choice of the parameter set $\mathbf{x} = (x_i)_{i=1,\dots,n}$ that defines the shape Γ can be done in several ways, which depend on the context. For wing shape parameterization, two sets of parameters are usually chosen, defining the shape characteristics first *globally*, and then *locally*. We consider here as testcase the wing of a typical business aircraft, whose baseline is described in [1].

In this study, the global characteristics of the wing shape are obtained from five parameters : the span, the root / tip chord length ratio, the angle of attack, the twist angle and the sweep angle, defined in Fig.(1). Modifications of these parameters are illustrated in Fig.(2) to Fig.(6)

The local characteristics of the wing shape are defined by imposing the section shape, which is constructed thanks to two cubic B-Spline curves, one for the suction side and one for the pressure side. Thus, the section shape is determined by 2×5 control points, which can be moved in crosswise direction. Control points located at leading edge and trailing edge are kept fixed. The section shape is the same for the whole wing. A random modification of three of these parameters is illustrated in Fig.(7).

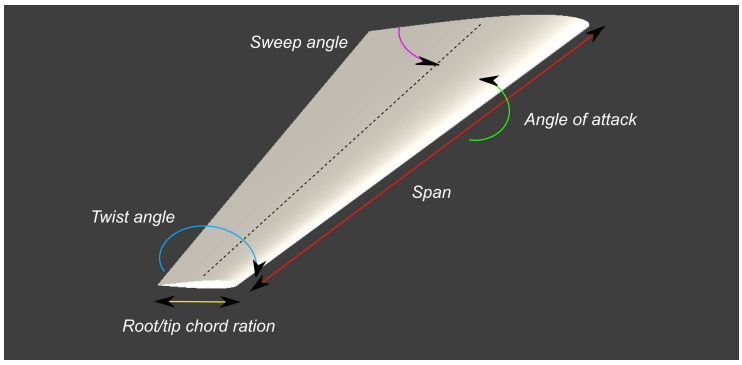

Figure 1: Parameters for global wing characteristics.

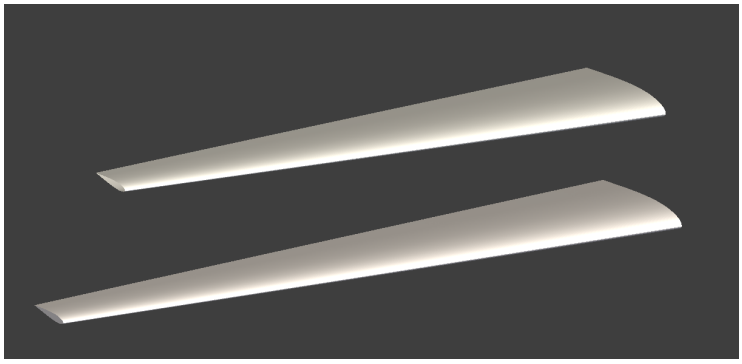

Figure 2: Illustration of span change.

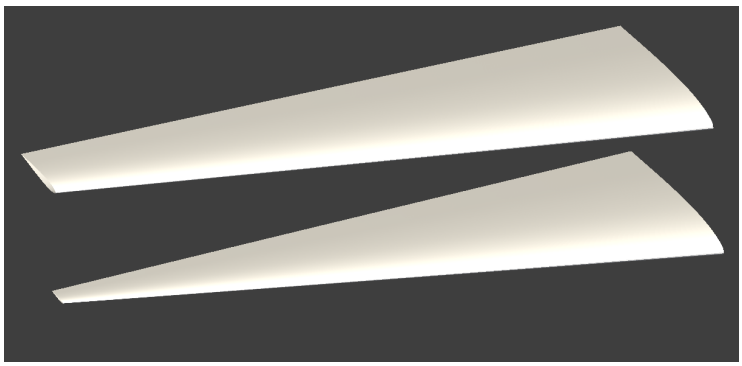

Figure 3: Illustration of root/tip chord length ratio change.

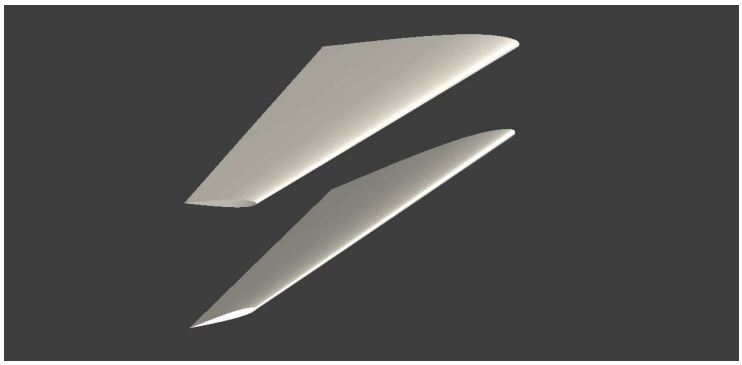

Figure 4: Illustration of angle of attack change.

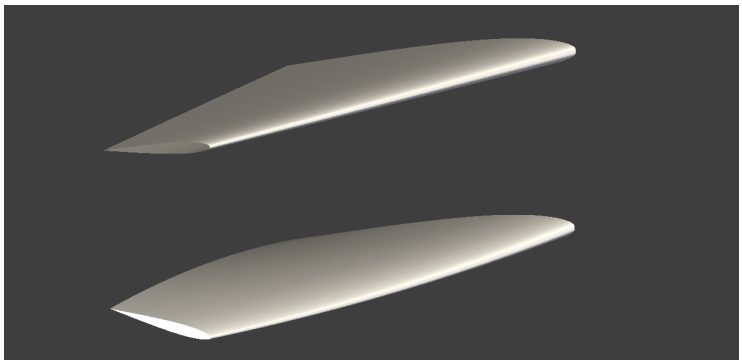

Figure 5: Illustration of twist angle change.

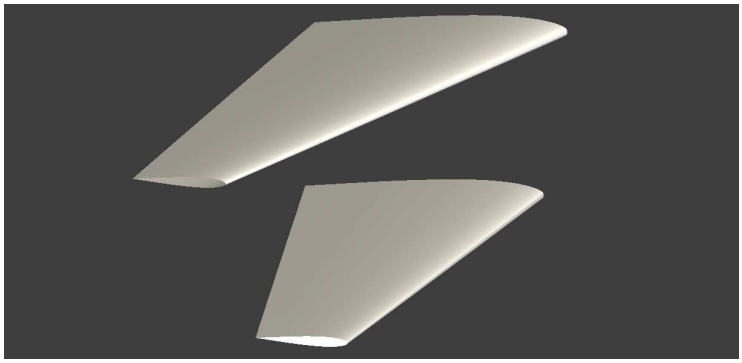

Figure 6: Illustration of sweep angle change.

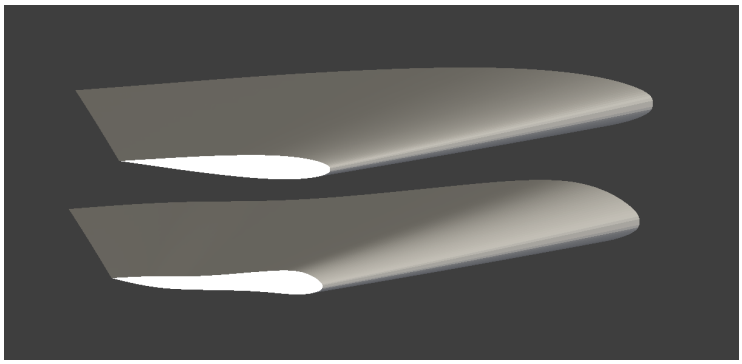

Figure 7: Illustration of local parameter change.

5 Single optimizations

The shape optimization algorithm presented above is carried out for three independent numerical experiments, considering successively only local shape parameters, only global shape parameters, and finally local and global shape parameters. Therefore, the number of optimization variables is successively $n = 10$, $n = 5$ and $n = 15$.

For each new parameter set provided by the optimizer, the wing shape is constructed automatically. When local shape parameters are optimized, global shape parameters are set according to the baseline wing shape, and vice versa. An unstructured grid, that counts approximatively 200 000 nodes, is then build for each new geometry using the GMSH grid generation software [4]. The state equations are then solved, as described above, using the NUM3SIS in-house parallel simulation platform [6].

The evolution of the cost function, for the three experiments performed, are plotted in Fig.(8). As can be seen, local shape optimization is very effective in this context, because a local shape change can reduce significantly the shock wave on the suction side of the wing. Fig.(9) and Fig.(10) illustrate the modification of the pressure field, whereas Fig.(13) shows the shape change, observed during the optimization of local shape parameters.

The optimization of global parameters yields a more limited drag reduction. When considering the pressure field plotted in Fig.(11), one can observe that the global shape change cannot reduce significantly the shock wave. However, the optimizer finds a global shape change that reduces the impact of the shock wave on the drag value. The shape change is represented in Fig.(14).

The result obtained by optimizing simultaneously local and global parameters is unexpected: The drag reduction is slightly better than that obtained with only global shape change, but far worse than that obtained with only local shape change. A better result is expected, since the design space generated by local shape change is included in the design space generated by local and global shape change. The observation of pressure field in Fig.(12) and shape change in Fig.(15) show that the optimizer has modified global and local shape parameters slightly, yielding a poor result. One may suppose that the mixing of global and local parameters leads to an optimization problem that exhibits several local minima, in which the optimizer is trapped.

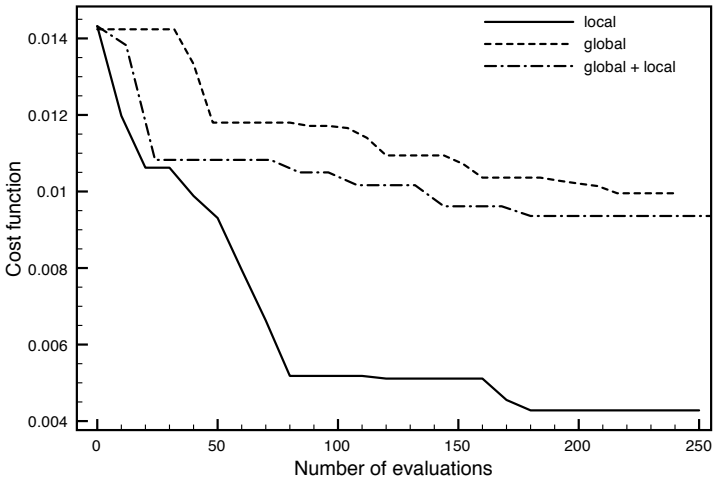

Figure 8: Evolution of the cost function for single optimizations.

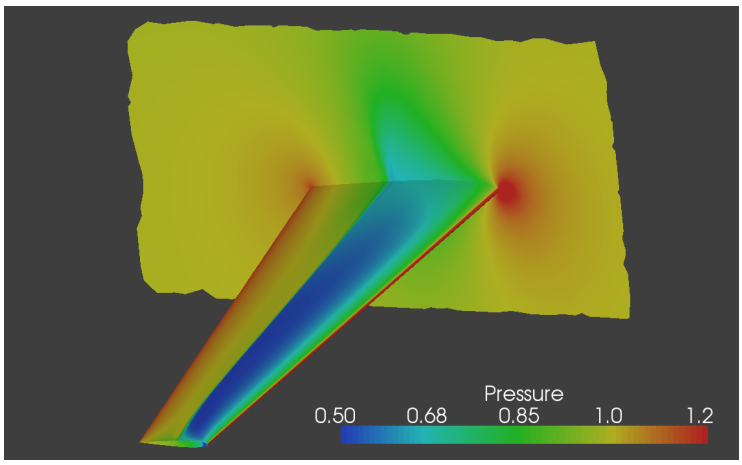

Figure 9: Pressure field for baseline shape.

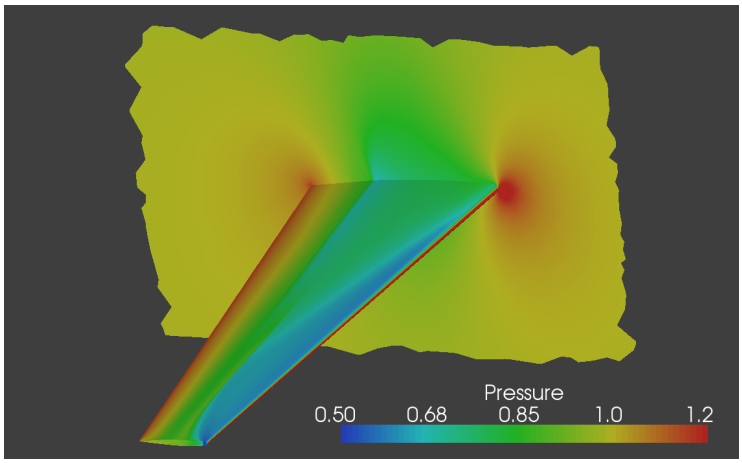

Figure 10: Pressure field for optimized local parameters.

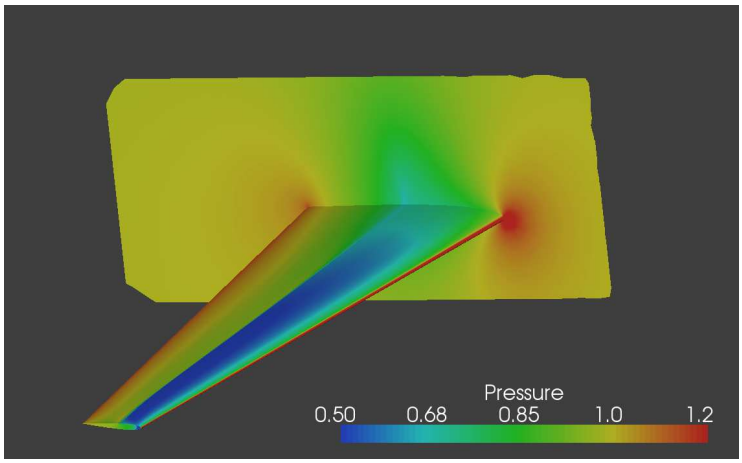

Figure 11: Pressure field for optimized global parameters.

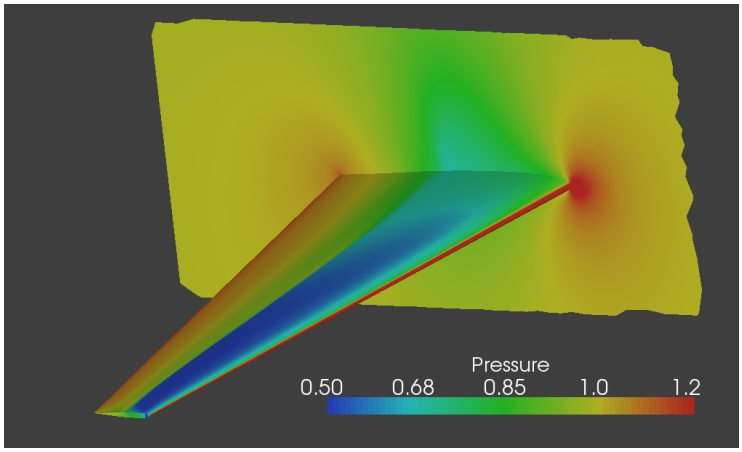

Figure 12: Pressure field for optimized global and local parameters.

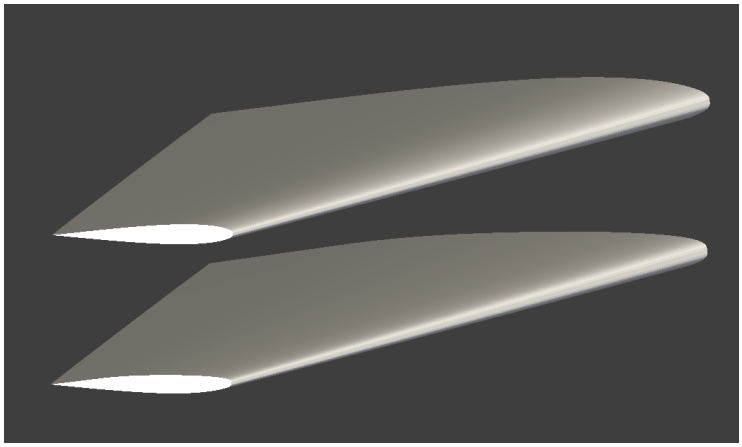

Figure 13: Comparison of wing shape : top baseline ; bottom : optimized local parameters.

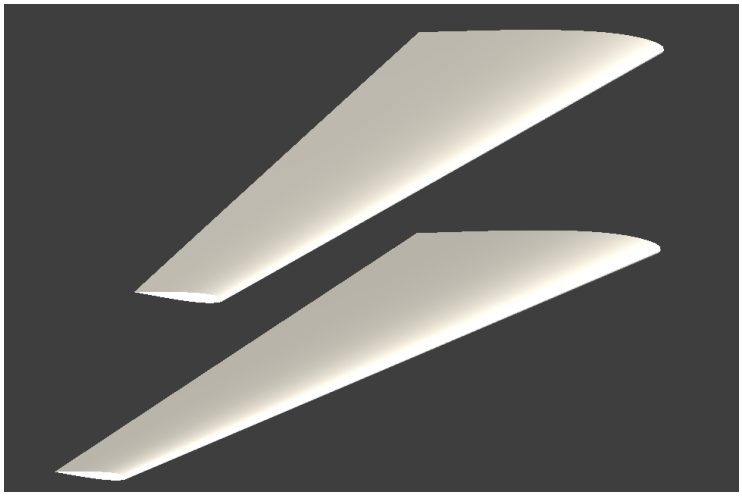

Figure 14: Comparison of wing shape : top baseline ; bottom : optimized global parameters.

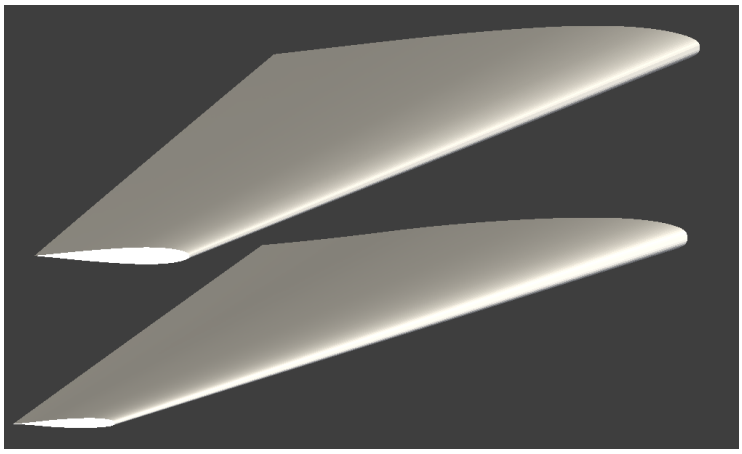

Figure 15: Comparison of wing shape : top baseline ; bottom : optimized global and local parameters.

6 Nested optimizations

Since a straightforward optimization including local and global shape changes fails, we consider other strategies. At first, we try a nested approach, that consists of two phases: in a first phase, only global shape parameters are optimized, yielding the global characteristics of the wing. This is then considered as a starting design for the second phase, during which local and global parameters are optimized. Actually, the first phase is just used to modify the initial point for the optimizer. We hope this can help to avoid being trapped in local minima.

The results obtained by carrying out this strategy on the selected testcase can be shown in Fig.(16). Starting from the design optimized with respect to global shape parameters leads to a better cost function value. However, this result is not better than that obtained using only local parameter changes. Moreover, the computational cost is significantly increased. This experiment shows that the design obtained by the optimization of global parameters is not a satisfactory starting point for the optimization of global and local parameters.

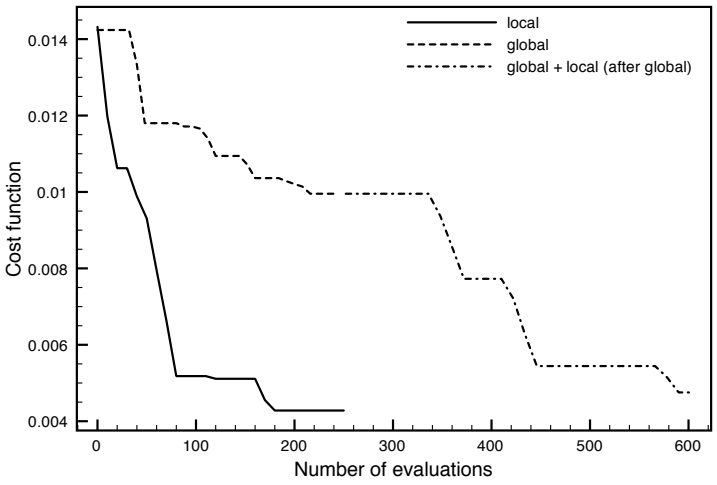

Figure 16: Evolution of the cost function for the nested optimizations approach.

7 Successive optimizations

A common practice in engineering design consists of optimizing successively global and local shape parameters. With such an approach, a first step aims at determining suitable global shape characteristics, whereas the second step modifies the shape obtained by local perturbations. This approach can be successful if the optimization problem is characterized by a so-called *separability* property. It means that the optimum can be reached by successive modifications of design variables.

This approach is thus tested, by optimizing the local shape parameters, after the global shape parameters have been optimized. Results are shown in Fig.(17). As can be seen, the cost function value reached is slightly better than the one obtained by a single optimization of local parameters. Nevertheless, this result is better than those obtained in previous experiments. This surprising result shows that optimizing separately local and global parameters is far more efficient than considering these variables as a whole.

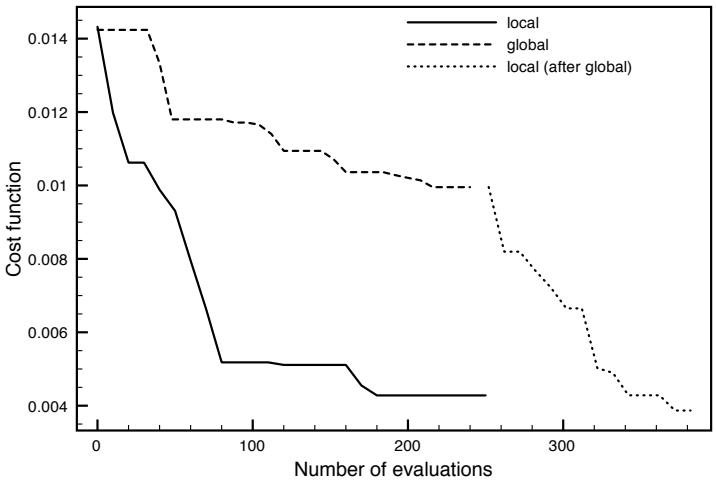

Figure 17: Evolution of the cost function for the successive optimizations approach.

8 Virtual game strategy

The previous experiment suggests the use of virtual Nash games, as a way to couple the optimizations of local and global shape parameters. Indeed, Nash games are based on the concept of *split of territories*, that consists of splitting the design variables in two sets, each set being optimized independently by a so-called *player*. Each player can have its own cost function to optimize. However, in our case, both players will have the same cost function, then we refer to *virtual* Nash games. In our context of local and global shape parameterization, the two sets will naturally correspond to the local $\mathbf{x}_l$ and global $\mathbf{x}_g$ parameter sets.

The algorithm employed can be summarized as:

1. choose a split of territories $\mathbf{x} = (\mathbf{x}_g, \mathbf{x}_l)$
2. choose initial design variables $\mathbf{x}^{(0)} = (\mathbf{x}_g^{(0)}, \mathbf{x}_l^{(0)})$;
   $k \leftarrow 0$;
3. begin iteration k' of the game loop ;
4. carry out in parallel K optimization iterations for each player :
   - first player updates $\mathbf{x}_g^{(k')}$ to $\mathbf{x}_g^{(k'+1)}$ with fixed $\mathbf{x}_l^{(k')}$;
   - second player updates $\mathbf{x}_l^{(k')}$ to $\mathbf{x}_l^{(k'+1)}$ with fixed $\mathbf{x}_g^{(k')}$;
5. synchronize the players : $\mathbf{x}^{(k'+1)} = (\mathbf{x}_g^{(k'+1)}, \mathbf{x}_l^{(k'+1)})$
6. finish iteration k' of the game loop ;
   if a stopping criterion is reached then STOP ;
   else $k' \leftarrow k' + 1$ GOTO step (2).

Such a strategy can reduce significantly the computational cost because each optimization is carried out in a design space of lower dimension and they can be solved in parallel, since they are independent. The described-above algorithm is carried out using only three iterations of the optimizer for each update achieved by the two players. The evolution of the cost function can be seen in Fig.(18). Using such a strategy, a better design is obtained for a computational cost similar to a single optimization.

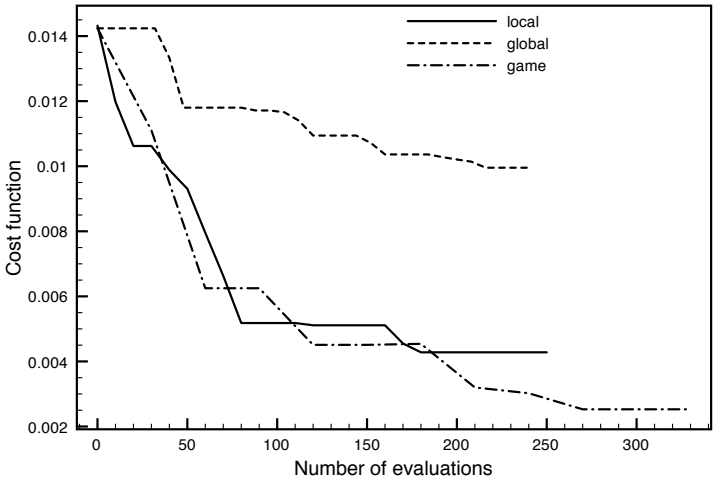

Figure 18: Evolution of the cost function for the game strategy.

9 Comparison of shapes and flows

We compare the local and global shape parameters in Tabs.(1-2), for the initial wing and wings obtained by single optimizations and game strategy. Obviously, the single optimization of global parameters and the game strategy yield shape modifications of opposite sign (except for the sweep angle). On the contrary, some similarities can be observed when comparing the shapes obtained using single optimization of local parameters and game strategy. This shows that the coupling of local and global parameters optimization modifies strongly the optimum global shape, but only slightly the optimum local shape.

Wing sections obtained can be compared in Figs.(19-22). As explained above, the section modification due to the coupling of the local and global parameters perturbes moderately the shape obtained by the optimization of local parameters only. A comparison of the shape for the initial wing and the wing optimized by Nash game is depicted in Fig.(23). The pressure field change is also represented in Fig.(24).

design variable	initial	global optimization	Nash game
span	2.59	2.49	2.75
root/tip ratio	0.3631	0.297	0.403
angle of attack	2.	2.272	1.899
twist angle	-1.	-0.775	-1.176
sweep angle	76.76	68.92	69.84

Table 1: Comparison of global parameters found.

design variable	initial	local optimization	Nash game
y_1^s	2	2.27	2.61
y_2^s	5	3.95	4.17
y_3^s	6	4.92	5.31
y_4^s	4	4.74	4.29
y_5^s	2	2.30	2.07
y_1^p	-2	-2.02	-1.67
y_2^p	-5	-4.47	-4.82
y_3^p	-6	-6.06	-5.36
y_4^p	-4	-4.04	-3.90
y_5^p	-2	-2.12	-1.82

Table 2: Comparison of local parameters found.

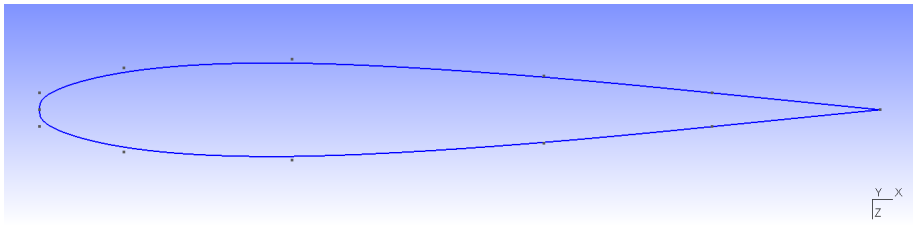

Figure 19: Initial wing section.

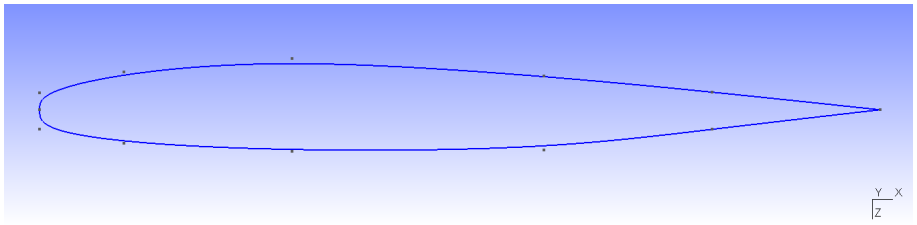

Figure 20: Wing section obtained with single optimization of local parameters.

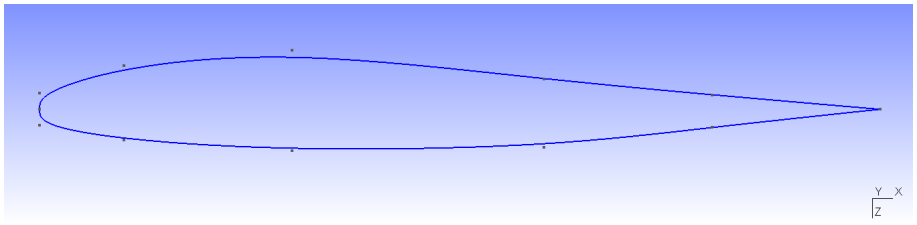

Figure 21: Wing section obtained with successive optimizations approach.

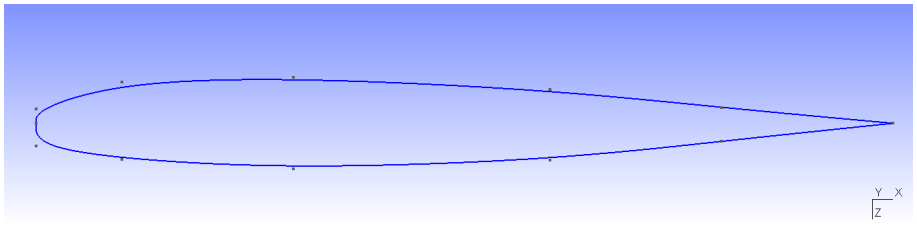

Figure 22: Wing section obtained with Nash game strategy.

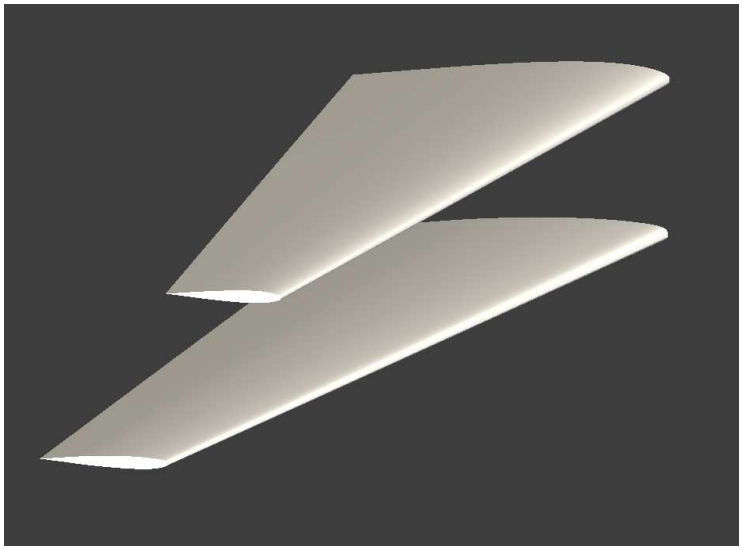

Figure 23: Comparison of the shape for the initial wing and the wing optimized by Nash game.

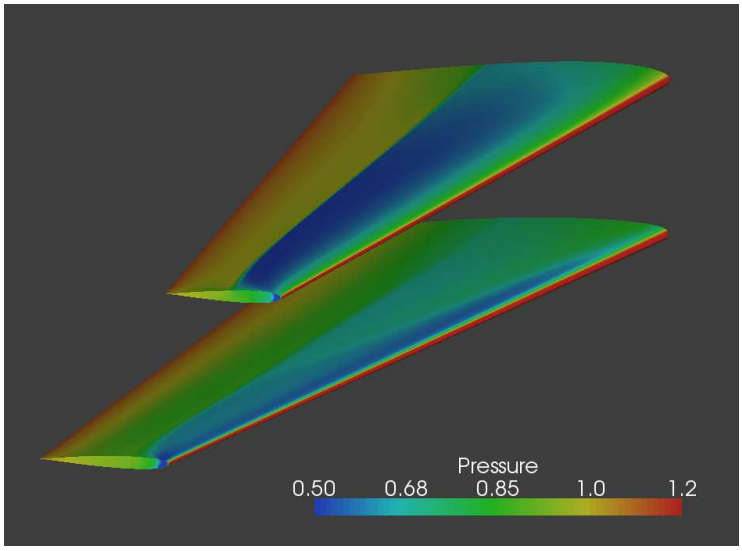

Figure 24: Comparison of the pressure field for the initial wing and the wing optimized by Nash game.

10 Conclusion

We have tested in this study various strategies to achieve the simultaneous optimization of both global and local wing shape parameters. In the case of a lift-constrained drag minimization, we have shown that a straightforward optimization fails due to multimodality, whereas a simpler approach, such as successive global and local shape optimizations provides not so bad results. This demonstrates that a separation of variables can somehow occurs. However, the use of virtual Nash games has been found more effective to couple local and global optimizations, yielding a better cost function value without increasing the computational cost.

References

[1] Andreoli, M., Janka, A., and Désidéri, J.-A. Free-form deformation parameterization for multilevel 3D shape optimization in aerodynamics. INRIA Research Report 5019, November 2003.

[2] Barth, T., and Jespersen, D. The design and application of upwind schemes on unstructured meshes. In *27th AIAA Aerospace Sciences Meeting, Reno, NV, 1989 (AIAA 89-0366)*.

[3] Batten, P., Clarke, N., Lambert, C., and Causon, M. On the choice of wavespeeds for the hllc Riemann solver. *SIAM J. Sci. Comput. 18*, 6 (November 1997), 1553–1570.

[4] Geuzaine, C., and Remacle, J.-F. Gmsh: a three-dimensional finite element mesh generator with built-in pre- and post-processing facilities. *Int. J. for Numerical Methods in Fluids 79*, 11 (2009), 1309–1331.

[5] Hansen, N., Muller, S., and Koumoutsakos, P. Reducing the time complexity of the derandomized evolution strategy with covariance matrix adaptation (cma-es). *Evolutionary Computation 11*, 1 (2003), 1–18.

[6] Kloczko, T. Concept, architecture and performance study for a parallel code in cfd. In *Parallel CFD Conference, May 19-22, Lyon, France.*

[7] Kloczko, T., Corre, C., and Beccantini, A. Low-cost implicit schemes for all-speed flows on unstructured meshes. *International Journal for Numerical Methods in Fluids 58*, 5 (October 2008), 493–526.

Contents

Centre de recherche INRIA Sophia Antipolis – Méditerranée
2004, route des Lucioles - BP 93 - 06902 Sophia Antipolis Cedex (France)

Centre de recherche INRIA Bordeaux – Sud Ouest : Domaine Universitaire - 351, cours de la Libération - 33405 Talence Cedex
Centre de recherche INRIA Grenoble – Rhône-Alpes : 655, avenue de l'Europe - 38334 Montbonnot Saint-Ismier
Centre de recherche INRIA Lille – Nord Europe : Parc Scientifique de la Haute Borne - 40, avenue Halley - 59650 Villeneuve d'Ascq
Centre de recherche INRIA Nancy – Grand Est : LORIA, Technopôle de Nancy-Brabois - Campus scientifique
615, rue du Jardin Botanique - BP 101 - 54602 Villers-lès-Nancy Cedex
Centre de recherche INRIA Paris – Rocquencourt : Domaine de Voluceau - Rocquencourt - BP 105 - 78153 Le Chesnay Cedex
Centre de recherche INRIA Rennes – Bretagne Atlantique : IRISA, Campus universitaire de Beaulieu - 35042 Rennes Cedex
Centre de recherche INRIA Saclay – Île-de-France : Parc Orsay Université - ZAC des Vignes : 4, rue Jacques Monod - 91893 Orsay Cedex

Éditeur
INRIA - Domaine de Voluceau - Rocquencourt, BP 105 - 78153 Le Chesnay Cedex (France)
http://www.inria.fr
ISSN 0249-6399